

## 1 Highlights

- 2 • We parameterize and validate a DEB model of *Pinna nobilis* accounting for metabolic acceleration.
- 3 • Ontogeny is captured well, and parameters are consistent with those of related species.
- 4 • Ontogeny of post-larval life stages is described well under the assumption of isometric growth.
- 5 • The model predicts growth and reproduction under various food and temperature conditions.
- 6 • Estimating food availability from individual sizes is plausible when food limits growth.

7 Dynamic energy budget of endemic and critically endangered bivalve *Pinna*  
8 *nobilis*: a mechanistic model for informed conservation

9 Ines Haberle<sup>a,\*</sup>, Nina Marn<sup>a,b</sup>, Sunčana Geček<sup>a</sup>, Tin Klanjšček<sup>a,\*</sup>

10 <sup>a</sup>Ruder Bošković Institute, Bijenička cesta 54, Zagreb HR-10002, Croatia

11 <sup>b</sup>School of Biological Sciences, The University of Western Australia, 35 Stirling Highway, Crawley, WA 6009, Australia

---

12 **Abstract**

The noble pen shell *Pinna nobilis* L. is the largest, endemic, critically endangered, and protected bivalve of the Mediterranean Sea. Effective conservation and management strategies for this species highly depend on understanding how environmental change and anthropogenic pressures, impact its physiology and thereby ecological function, population persistence, and survival. Dynamic Energy Budget (DEB) theory offers a valuable mechanistic modelling framework for capturing how an organism acquires and utilizes available energy for growth, maturation, development and reproduction throughout its life cycle, while accounting for environmental conditions. In this study we parameterized and compared two types of DEB models using limited literature data: a standard model that accounts for morphological metamorphosis only, and a model that through metabolic acceleration between birth and metamorphosis captures physiological changes occurring in the larval life stage. The model with metabolic acceleration performed better, successfully simulating life history traits, growth, and reproduction of *P. nobilis*. We used the model to predict how food availability implemented through functional response affects growth, maturation, and reproduction of the species throughout its lifespan. We found that (i) abundant food had little effect on the size at maturation, (ii) maximum fecundity at ultimate age doubled compared to typically lower food availability in the wild, (iii) puberty could not be reached below the food availability corresponding to functional response value of 0.164, and (iv) energy allocated to reproduction was positively correlated with both bivalve size and food availability. Accounting for allometric growth observed in *P. nobilis* did not affect the findings, prompting us to recommend that isometric growth be assumed when modelling the bivalve using DEB. The model presented here is the first full-life cycle bioenergetic model made for *P. nobilis*. It can be used standalone for predicting energy budget of individuals at specific environmental conditions, or as a building block for modeling populations and ecosystems under various environmental scenarios. The model can readily incorporate other environmental factors relevant to changes in physiology and energy allocation, such as oxygen and pH.

13 **Keywords:** Noble pen shell, Dynamic Energy Budget (DEB) theory, Parameter estimation, Life  
14 history, Food availability, Conservation

---

\*Corresponding authors

Email addresses: [ines.haberle@irb.com](mailto:ines.haberle@irb.com) (Ines Haberle), [tin@irb.com](mailto:tin@irb.com) (Tin Klanjšček)

## 15 1. Introduction

16 The noble pen shell *Pinna nobilis* (Linnaeus, 1758) is the largest endemic bivalve of the Mediterranean  
17 Sea. Initially collected for its meat, byssus threads, and as a souvenir, the bivalve has also been impacted  
18 by other human activities such as boat anchoring, coastal construction, and illegal trawling (Katsanevakis  
19 et al., 2011; Deudero et al., 2015; Basso et al., 2015b). Despite being protected in Croatia since 1977  
20 and Europe-wide since 1992 (EU Directive 92/43/EEC, Barcelona Convention Annex II), *P. nobilis* has  
21 been experiencing an accelerated decline, culminating with mass mortality events due to parasite infec-  
22 tions that started in 2016 (Vázquez-Luis et al., 2017; Cabanellas-Reboredo et al., 2019; Carella et al.,  
23 2019). Consequently, in October 2019, conservation status of *P. nobilis* was updated from endangered to  
24 critically endangered (Kersting et al., 2019). As an immediate action, several Mediterranean institutions  
25 started *ex situ* conservation programs focused on captive breeding and reintroduction (Kersting et al.,  
26 2019; Prado et al., 2019), with additional emphasis on preserving still intact wild populations. To be  
27 effective, such conservation programs require understanding of how environmental changes and anthro-  
28 pogenic pressures impact physiology of the species, and thereby their ecological function, population  
29 persistence, and survival (Seebacher and Franklin, 2012). The idea of integrating physiology perspective  
30 into conservation was conveniently summarized under the term *conservational physiology* (Wikelski and  
31 Cooke, 2006; Cooke et al., 2013).

32 Mechanistic predictive models play a significant role in conservational physiology by predicting how  
33 various scenarios of environmental change affect organisms and populations, thus informing conservation  
34 planning (Urban et al., 2016; Ijima et al., 2019; Marn et al., 2020). Individual-level bioenergetic models  
35 are especially valuable because they reveal how the organisms use currency of life - energy - for various  
36 physiological processes across a range of environmental scenarios.

37 Bioenergetic models based on Dynamic energy budget (DEB) theory (Kooijman, 2010) benefit from  
38 a particularly flexible parameterization: while only limited data is *necessary*, a wide range of data types  
39 and sources *can* be assimilated. DEBtool, a specialized DEB parameter estimation tool, facilitates  
40 assimilation by mostly automatizing the parameter estimation procedure (Lika et al., 2011; Marques  
41 et al., 2019). A well parameterized DEB model interconnects fundamental life processes of an individual  
42 - energy assimilation, growth, development, maintenance, and reproduction - at all life stages, while  
43 accounting for a dynamic environment (Sousa et al., 2008; Nisbet et al., 2012). If we assume that the  
44 idealized individual - i.e., one holding average characteristics - is representative of a population, then  
45 gaining insight into its complex energy dynamics enables assessment of population-level response to a  
46 range of environmental conditions.

47 In this study we parameterize a DEB model of *Pinna nobilis* using growth and reproduction data  
48 available from the literature. Following an introduction of biology and ecology of *P. nobilis* and overview  
49 of the DEB modelling approach, we provide a description of data used for parameterization. We then

50 present model parameters and the model validation, and discuss physiological implications of the results  
51 focusing on growth and reproductive output as a function of food availability. We end by discussing a pos-  
52 sibility of scaling up the DEB model to be used as a building block for modeling impacts of environmental  
53 change on higher levels of biological organisation.

## 54 **2. Material and Methods**

### 55 *2.1. Biology and ecology of *P. nobilis**

56 The noble pen shell *Pinna nobilis* is one of the largest and long -living bivalves worldwide, reaching up  
57 to 120 cm in length (Zavodnik et al., 1991) and more than 27 years of age (Galinou-Mitsoudi et al., 2006;  
58 Rouanet et al., 2015). It has been endemic to the Mediterranean Sea since Miocene, occupying coastal  
59 areas up to 60m of depth (Gómez-Alba, 1988; Zavodnik et al., 1991). Associated with soft sediments, it  
60 inhabits primarily seagrass meadows or bare sand, where it is partially buried and fixed in the substrate,  
61 with the posterior end projected into the water column (Šiletić and Peharda, 2003; Katsanevakis, 2005;  
62 Marin et al., 2011).

63 *P. nobilis* is a successive hermaphrodite, developing both male and female gonads and experiencing  
64 asynchronous gamete maturation (Deudero et al., 2017). The gonad development starts in early spring,  
65 followed by the spawning season during summer (De Gaulejac, 1993; Richardson et al., 1999). *P. nobilis*  
66 undergoes the classical bivalve development, starting of as a larvae that initiates feeding after two days,  
67 and settles within 10 days (Trigos et al., 2018). The settlement usually occurs in late summer and early  
68 autumn (Butler et al., 1993). Once settled, the individual grows rapidly and typically reaches sexual  
69 maturity by the age of two years (Butler et al., 1993; Richardson et al., 1999). The reproduction and  
70 recruitment potential vary between years (Peharda et al., 2012; Vafidis et al., 2014) because they depend  
71 on pre-spawning state of the adult (Cabanellas-Reboredo et al., 2009), and are strongly influenced by  
72 environmental conditions.

73 *P. nobilis* has two major ecological roles: (i) as a large filter feeder, it contributes to water clar-  
74 ity by retaining substantial amounts of detritus and organic matter (Trigos et al., 2014), and (ii) it  
75 supports biodiversity of soft-bottom areas by providing hard substrate and shelter for other benthic  
76 organisms (Garcia-Marsh and Vicente, 2006; Basso et al., 2015b). Due to its susceptibility to various  
77 pressures, *P. nobilis* also serves as an important bio-indicator of health status for Mediterranean ecosys-  
78 tems (Cabanellas-Reboredo et al., 2019).

### 79 *2.2. Application of DEB theory to *P. nobilis**

80 We used Dynamic Energy Budget (DEB) theory (Sousa et al., 2008; Kooijman, 2010; Jusup et al.,  
81 2017) to model the energy budget and life cycle of *P. nobilis*. The theory describes and quantifies the  
82 flow of mass and energy within the organism by obeying thermodynamic principles. Contrary to other

83 available bioenergetic models, DEB models describe the organism’s energy budget throughout the whole  
84 life cycle, from embryonic to adult life stages, while accounting for impact of environmental conditions  
85 (primarily temperature and food) on physiological processes (Kooijman, 2010; Jusup et al., 2017).

86 DEB theory applies to all life on Earth and, to accommodate special requirements of specific taxa  
87 such as extra life stage or metabolic change, it allows for the construction of variety of typified DEB  
88 models (Marques et al., 2018). All typified models are variations on the standard DEB model, with state  
89 variables and energy fluxes following the same basic concept, albeit including additional processes and  
90 the related parameters. Choosing the typified model, or otherwise extending the basic model should be  
91 based on insights into physiological characteristics of the species. If the insights are lacking, then using  
92 the simplest model that yields satisfactory results is the conservative approach that minimizes overfitting.

93 To model *P. nobilis*, two specific ontogeny characteristics need to be considered: possible metabolic  
94 change at metamorphosis, and allometric growth after metamorphosis. Because available data are in-  
95 sufficient to a-priori identify the more appropriate model, we parameterized different variants of the  
96 DEB model. First, we compared the standard DEB model to a model accounting for metabolic change  
97 assuming isometric growth. Following the comparison, we investigated the effects of allometric growth.

98 **Standard DEB model.** The standard (*std*) DEB model divides organism into compartments described  
99 by 4 state variables: energy reserve ( $E$ ), structure ( $V$ ), maturity ( $E_H$ ), and reproduction buffer ( $E_R$ )  
100 (Fig. 1). The energy flow through the organism is tracked by specifying energy fluxes. Energy is ingested  
101 ( $\dot{p}_X$ ) through feeding, assimilated into reserve ( $\dot{p}_A$ ), and mobilized for physiological processes ( $\dot{p}_C$ ). A  
102 fixed fraction ( $\kappa$ ) of energy is mobilized to somatic branch, where it is used for maintaining current  
103 structure of the organism (somatic maintenance,  $\dot{p}_S$ ) and for somatic growth ( $\dot{p}_G$ ). Remaining fraction  
104 ( $1-\kappa$ ) is allocated into reproductive branch, where it is spent on maintaining developmental complexity of  
105 the organism (maturity maintenance,  $\dot{p}_J$ ), and maturation before - or reproduction after - the organism  
106 becomes an adult ( $\dot{p}_R$ ). Once defined, the energy fluxes determine differential equations guiding the  
107 dynamics of state variables (Table 1).

108 State variables of the DEB model in principle cannot be measured directly, and need to be related  
109 to observable quantities where possible. Structural volume,  $V$ , is a cube of structural length,  $L$ , and is  
110 related to physical length of the organism,  $L_w$ , through an auxiliary parameter shape coefficient,  $\delta_M$ :

$$L = \delta_M L_w \tag{1}$$

111 The physical length has to be carefully chosen to accurately represent the size of the organism, and has  
112 to be independent of energy reserves and/or reproductive buffer (i.e., fatness).

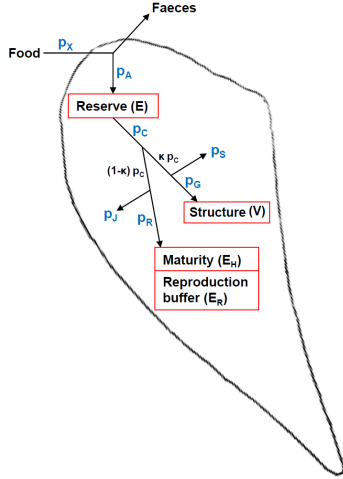


Figure 1: Schematic representation of a DEB model with associated state variables (boxes) and energy fluxes (arrows). State variables: reserve ( $E$ ), structure ( $V$ ), maturity ( $E_H$ ), reproduction buffer ( $E_R$ ). Energy fluxes:  $\dot{p}_X$  - ingestion,  $\dot{p}_A$  - assimilation,  $\dot{p}_C$  - mobilization,  $\dot{p}_S$  - somatic maintenance,  $\dot{p}_G$  - growth,  $\dot{p}_J$  - maturity maintenance,  $\dot{p}_R$  - maturation/reproduction. A fixed fraction of energy,  $\kappa\dot{p}_C$ , is mobilized into somatic branch, while the remaining energy,  $(1-\kappa)\dot{p}_C$ , goes to reproductive branch.

113 As most bivalves, *P. nobilis* undergoes a larval life stage and metamorphoses into an adult bivalve.  
 114 Hence, at least two measures of physical length are needed to describe the organism: the larvae diameter  
 115 before, and shell length after metamorphosis. The morphological transformation from one stage to the  
 116 other is captured using an additional shape coefficient corresponding to larval shape.

117 **Metabolic change at metamorphosis.** Life history traits of *P. nobilis* suggest that a change in  
 118 morphology may not be sufficient to explain substantial adaptations required for changing from a free-  
 119 drifting planktonic to a sessile benthic way of life. We hypothesize that metamorphosis of *P. nobilis* may  
 120 also involve a metabolic change that cannot be captured by the *std* model; a typified *abj* model should  
 121 be used instead (Kooijman, 2014; Marques et al., 2018).

122 The typified *abj* model is a one-parameter extension of the above described *std* model that, alongside  
 123 the extra shape coefficient to address larvae shape, also includes an acceleration factor,  $s_M$ , accounting  
 124 for metabolic acceleration between birth and metamorphosis. Acceleration factor increases from unity at  
 125 birth to its maximum value at metamorphosis, and thereafter remains constant, equal to ratio of length  
 126 at metamorphosis  $L_j$ , and length at birth  $L_b$ :

$$s_M = \frac{L_j}{L_b} \quad (2)$$

127 Acceleration factor increases values from birth to metamorphosis of two primary parameters: surface-  
 128 specific maximum assimilation rate  $\{\dot{p}_{Am}\}$  and energy conductance  $\dot{v}$ . The increase, in turn, affects  
 129 energy fluxes determining the dynamics of state variables (Table 1).

Table 1: Energy fluxes and state variables of the standard (*std*) and typified *abj* DEB models. The *abj* model is a one-parameter extension of the *std* model - acceleration factor  $s_M$  (indicated in bold) affects assimilation ( $\dot{p}_A$ ) and mobilisation ( $\dot{p}_C$ ) energy fluxes. Even though dynamics is impacted by the differences in  $\dot{p}_A$  and  $\dot{p}_C$ , both models share general mathematical expressions for ingestion ( $\dot{p}_X$ ), growth ( $\dot{p}_G$ ) and maturity/reproduction ( $\dot{p}_R$ ), and state variables reserve ( $E$ ) and structure ( $V$ ). Somatic and maturity maintenance ( $\dot{p}_S$ ,  $\dot{p}_J$ ), and state variables maturity ( $E_H$ ) and reproduction ( $E_R$ ), are not impacted by the acceleration. The list of model parameters is presented in Table A.1 and Table 3, for the *std* and typified *abj* model, respectively.

Energy flux	<i>std</i>	<i>abj</i>
Ingestion		$\dot{p}_X = \frac{\dot{p}_A}{\kappa_X}$
Assimilation	$\dot{p}_A = \{\dot{p}_{Am}\} f L^2$	$\dot{p}_A = \{\dot{p}_{Am}\} \mathbf{s}_M f L^2$
Mobilization	$\dot{p}_C = E \frac{\dot{v}[E_G]L^2 + \dot{p}_S}{\kappa E + [E_G]L^3}$	$\dot{p}_C = E \frac{\dot{v}\mathbf{s}_M[E_G]L^2 + \dot{p}_S}{\kappa E + [E_G]L^3}$
Somatic maintenance		$\dot{p}_S = [\dot{p}_M]L^3$
Growth		$\dot{p}_G = \kappa \dot{p}_C - \dot{p}_S$
Maturity maintenance		$\dot{p}_J = \dot{k}_J E_H$
Maturity/Reproduction		$\dot{p}_R = (1 - \kappa)\dot{p}_C - \dot{p}_J$
State variable	<i>std</i> and <i>abj</i>	
Reserve	$\frac{dE}{dt} = \dot{p}_A - \dot{p}_C$	
Structure	$\frac{dV}{dt} = \frac{\dot{p}_G}{[E_G]}$	where $V = L^3$
Maturity	$\frac{dE_H}{dt} = \dot{p}_R$	if $E_H < E_H^p$ else $\frac{dE_H}{dt} = 0$
Reproduction	$\frac{dE_R}{dt} = \kappa_R \dot{p}_R$	if $E_H \geq E_H^p$ else $\frac{dE_R}{dt} = 0$

130 **Allometric growth.** In this study we initially assume that *P. nobilis* has isometric growth both before  
131 and after metamorphosis. However, according to Katsanevakis et al. (2007), the shell of *P. nobilis* exhibits  
132 allometric growth best described using two-segment allometric model with a breakpoint at the length of  
133 20 cm. Up to the breakpoint, relative growth of width in relation to length is strongly positive, i.e. the  
134 bivalve preferentially widens, while thereafter the allometry becomes negative, and the bivalve elongates.  
135 In order to investigate whether allometric growth impacts the physiological energetics of the bivalve,  
136 we parameterized an additional *abj* model accounting for allometric growth as described in detail in  
137 Appendix C.

138 **Environmental factors.** Both *std* and *abj* models incorporate impacts of two environmental factors,  
139 temperature and food, on physiological processes. This allows inclusion of multiple data sets collected  
140 under various environmental and laboratory conditions into single parameterization process. Effects of  
141 environmental temperature are incorporated as a correction factor based on the Arrhenius expression

$$TC = \exp\left(\frac{T_A}{T_{ref}} - \frac{T_A}{T}\right) \quad (3)$$

142 where  $T_A$  is the Arrhenius temperature,  $T_{ref}$  is the reference temperature, and  $T$  is the environmental  
 143 temperature. The factor is applied by multiplying physiological rates given at  $T_{ref}$  with the expression Eq.  
 144 3. We calculated Arrhenius temperature of *P. nobilis* using growth rate-temperature relation reported by  
 145 Richardson et al. (1999). The correction applies to: assimilation  $\{\dot{p}_{Am}\}$ , energy conductance  $\dot{v}$ , specific  
 146 volume-linked somatic maintenance rate  $[\dot{p}_M]$ , and maturity maintenance rate coefficient  $\dot{k}_J$ . Response to  
 147 environmental food availability is incorporated as a Holling type-II functional response  $f$  that quantifies  
 148 amount of food available, ranging from 0 (no food) to 1 (unlimited food):

$$f = \frac{X}{X + K} \quad (4)$$

149 where  $X$  is the environmental food concentration, and  $K$  the half-saturation constant.

### 150 2.3. Empirical data for parameterization and validation

151 For parameterization and validation of the models we gathered empirical data from literature. The  
 152 same data were used to parameterize all models. Data points representing information on life history traits  
 153 such as age and length at specific life events (birth, metamorphosis, puberty, ultimate) and reproduction  
 154 (gonadosomatic index - GSI, energy of an egg) are given in Table 2 (column 4). DEBtool refers to  
 155 these type of data as *zero-variate* data. Various time series and other series of data (e.g. growth rate vs.  
 156 length) constitute *uni-variate* data in DEB. We used uni-variate data on (i) average length vs. age for two  
 157 populations, length vs. time of two young individuals (1 and 2 year old), and growth rate vs. temperature  
 158 from Richardson et al. (1999); (ii) growth rate vs. length from Šiletić and Peharda (2003); and (iii)  
 159 fecundity vs. length data from laboratory experiments performed by Trigos et al. (2018). All data were  
 160 extracted from graphs using PlotReader freeware (<https://jornbr.home.xs4all.nl/plotreader/>).

161 Data were accompanied with information on corresponding environmental temperature and functional  
 162 response  $f$  representing food availability. Initial value of  $f$  for each sampling site was estimated according  
 163 to Marn et al. (2017), as a ratio of site-specific ultimate size (the largest individual ever reported for  
 164 respective sampling site), and the size of the largest individual ever reported, i.e. 120 cm (Zavodnik et al.,  
 165 1991), which we assume to represent maximum size for the species at abundant food  $f = 1$ . Because such  
 166 estimates are not as reliable as measurements, we let  $f$  adjust itself during parameterization. Value of  
 167  $f$  for assimilation of zero-variate data was similarly calculated by dividing the common ultimate size of  
 168 the species in the wild, 86 cm (Richardson et al., 1999), by the largest observed size of 120 cm. Value of  
 169  $f$  for laboratory data was fixed to 1, assuming *ad libitum* feeding. All values of  $f$  are given in Table 4.

170 Model was validated using an independent length vs. time dataset from an *in situ* growth experiment  
 171 reported by Kožul et al. (2012) with temperature data for the respective area taken from Peharda et al.  
 172 (2012), and corresponding estimation of functional response value.

Table 2: Observed and fitted life history traits of *Pinna nobilis* using typified *abj* model, at functional response value  $f = 0.72$ . References denote the sources of observed data. RE represents relative error of the fitted values. Goodness of fit statistics: MRE = 0.202; SMSE = 0.194.

Data	Unit	Reference	Observed	Fitted	RE
Age at birth	d	Trigos et al. (2018)	2	1.98	0.01
Age at metamorphosis	d	Butler et al. (1993)	10	7.05	0.29
Age at puberty	y	Richardson et al. (1999)	1.5	1.26	0.15
Lifespan	y	Galinou-Mitsoudi et al. (2006)	27	27	<0.01
Size at birth	cm	Trigos et al. (2018)	0.0085	0.0085	<0.01
Length at metamorphosis	cm	Butler et al. (1993)	0.1	0.23	1.28
Length at puberty	cm	Deudero et al. (2017)	16.5	20.18	0.22
Ultimate shell length	cm	Richardson et al. (1999)	86	79.82	0.07
Initial energy of an egg	J	van der Veer et al. (2006)	0.001*	0.001	0.02
Gonadosomatic index (GSI)	-	Deudero et al. (2017)	0.52	0.48	0.08

\* Data for *Crassostrea gigas*

#### 173 2.4. Parameter estimates and goodness of fit

174 We used DEBtool package ([https://add-my-pet.github.io/DEBtool\\_M/](https://add-my-pet.github.io/DEBtool_M/)) in Matlab R2011b to  
175 estimate parameters of both *std* and typified *abj* *P. nobilis* DEB models, as well as the *abj* model  
176 accounting for allometric growth. The estimation process follows a co-variation method which, based  
177 on the provided data, aims to find a parameter set that minimizes the difference between predicted  
178 and observed values using a Nelder-Mead search algorithm (Lika et al., 2011; Marques et al., 2019). The  
179 parameterization requires initial values of primary parameters to facilitate start of the estimation process,  
180 but do not constrain the final result. The initial values were either parameter values of related species, if  
181 available, or of a generalized animal at the reference temperature (20°C) (Kooijman, 2010).

182 The obtained parameter set was evaluated for goodness of fit by computing Mean Relative Error  
183 (MRE) and Symetric Mean Square Errors (SMSE). The values lie in the interval  $[0, \infty)$  and  $[0, 1]$ , re-  
184 spectively, where 0 indicates exact match between observed data and their predictions. To assign the  
185 completeness of the real data we followed guidelines in Lika et al. (2011).

#### 186 2.5. Predicting impact of food availability on reproduction

187 Using the parameterized *abj* typified DEB model, we predicted the impact of food availability on  
188 the energy invested in growth, maturity and reproduction. Predictions were carried out for the common  
189 lifespan of *P. nobilis* (27 years), and for four food levels. Abundant food scenario was set as  $f = 1$ ,  
190 common food level of wild populations was  $f = 0.72$ , and the lowest food scenario of  $f = 0.16$  was selected  
191 as the highest  $f$  that did not support reproduction. An additional  $f = 0.3$  was selected arbitrarily between

192 the lowest and the common value to represent how lower food level affects organism that reproduces. We  
193 also predicted the combined effect of food availability and bivalve size on the amount of energy allocated  
194 to reproduction and the number of produced eggs (fecundity). To obtain the fecundity, we first multiplied  
195 the amount of energy accumulated in the reproductive buffer by the egg conversion efficiency  $\kappa_R$ , and  
196 then divided the result by the corresponding initial reserve of an egg for each food level.

### 197 3. Results

198 Estimated parameters of both *std* (Table A.1) and typified *abj* (Table 3) DEB models provided a good  
199 fit between the observations and the model outputs of *Pinna nobilis* traits. Overall performance of the  
200 *abj* model was better, resulting in more realistic simulations of life history traits (Table 2 vs. Table A.2)  
201 and growth of the species (Fig. 2a vs. Fig. A.1a).

202 Inclusion of the allometric growth into the *abj* model had minor impact on the parameter values,  
203 with largest effects on energy thresholds of life stages, and the shape coefficient after metamorphosis  
204 (Table C.1). Estimates of age, length at puberty, and ultimate length (data not shown) were closer to  
205 the values used for parameterization compared to the estimates obtained with the typified *abj* model.  
206 However, the allometric model had lower overall goodness of fit despite higher complexity and three  
207 additional parameters (MRE: 0.212 vs. 0.202; SMSE: 0.201 vs. 0.194; with vs. without allometry,  
208 respectively).

209 According to Lika et al. (2011), completeness of real data used for parameterization was 3 out of 10,  
210 among the top 3% in the AmP species database. Hereafter, we present results of the typified *abj* model,  
211 while the full results of the *std* model and the *abj* model accounting for allometric growth are given in  
212 Appendix A and Appendix C, respectively.

#### 213 3.1. Model parameters

214 Shape coefficients, 0.611 and 0.066 for pre- and post metamorphosis phase, respectively, represent  
215 the change from spherical to elongated shape very well. The acceleration factor  $s_M$  accelerates initial  
216 metabolism to almost 3-fold at metamorphosis, with surface-specific assimilation rate  $\{\dot{p}_{Am}\}$  reaching  
217  $101.44 \text{ J d}^{-1} \text{ cm}^{-2}$ , and energy conductance  $\dot{v}$  increasing to  $0.026 \text{ cm d}^{-1}$ . Allocation to soma  $\kappa = 0.53$   
218 implies that the energy is almost equally divided between the somatic and reproductive branches. The  
219 volume-specific cost of structure  $[E_G] = 2362 \text{ J cm}^{-3}$  is close to the median value of  $2357 \text{ J cm}^{-3}$  for the  
220 bivalves (AmP-collection, 2020), while the volume-specific maintenance cost  $[\dot{p}_M]$  of  $7.299 \text{ J d}^{-1} \text{ cm}^{-3}$  is  
221 somewhat at the low end, but still in the range reported for other bivalves ( $0.49\text{-}51.68 \text{ J d}^{-1} \text{ cm}^{-3}$  with an  
222 outlier of  $136.5 \text{ J d}^{-1} \text{ cm}^{-3}$ , 50 species). Maturity at puberty is relatively high, which is not rare for a long-  
223 living organism. The self-adjusted values of functional responses did not differ considerably from initially  
224 estimated values, except for one sampling site where the initial value was underestimated (Table 4).

Table 3: Parameter estimates of typified *abj* DEB model for *Pinna nobilis* at the reference temperature  $T_{ref} = 20^\circ\text{C}$ . Fixed parameters ( $\kappa_X$ ,  $\kappa_R$ ,  $F_m$ ,  $T_{ref}$ ,  $T_A$ ) are indicated in bold.

Parameter	Symbol	Value	Unit
Maximum surface-specific assimilation rate	$\{\dot{p}_{Am}\}$	34.74 (101.44)*	$\text{J d}^{-1} \text{cm}^{-2}$
Fraction of food energy fixed in reserve	$\kappa_X$	<b>0.80</b>	–
Allocation fraction to soma	$\kappa$	0.53	–
Reproduction fraction fixed in eggs	$\kappa_R$	<b>0.95</b>	–
Maximal surface-specific searching rate	$F_m$	<b>6.5</b>	$\text{l d}^{-1} \text{cm}^{-2}$
Energy conductance	$\dot{v}$	0.0089 (0.026)*	$\text{cm d}^{-1}$
Volume-specific somatic maintenance rate	$[\dot{p}_M]$	7.299	$\text{J d}^{-1} \text{cm}^{-3}$
Volume specific costs of structure	$[E_G]$	2362	$\text{J cm}^{-3}$
Maturation threshold for birth	$E_H^b$	$2.9 \cdot 10^{-04}$	J
Maturation threshold for metamorphosis	$E_H^j$	$7.3 \cdot 10^{-03}$	J
Maturation threshold for puberty	$E_H^p$	5601	J
Maturity maintenance rate coefficient	$\dot{k}_J$	0.002	$\text{d}^{-1}$
Zoom factor	$z$	2.52	–
Shape coefficient (larvae)	$\delta_{M1}$	0.611	–
Shape coefficient (adult)	$\delta_{M2}$	0.066	–
Acceleration factor	$s_M$	2.92	–
Reference temperature	$T_{ref}$	<b>293.15</b>	K
Arrhenius temperature	$T_A$	<b>9002</b>	K

\* The value in the brackets is the parameter value after metamorphosis (affected by  $s_M$ ).

Table 4: Initial estimates and fitted site-specific values of functional responses  $f$  using a typified *abj* model for *Pinna nobilis*. Values of  $f$  were estimated under the assumption that food limits growth, as the ratio between site-specific ultimate size and the largest *P. nobilis* individual ever reported\*. If not indicated differently, the site-specific ultimate size was taken from the corresponding reference (column 5).  $f$  was not fitted for zero-variate, laboratory, and validation data sets. The estimation procedure works well for 3 out of 4 localities, but fails for a locality with high anthropogenic influence, where size may not be limited by food (locality with estimate  $f = 0.38$ ).

Site no.	Dataset	Estimated $f$	Fitted $f$	Reference
-	Zero-variate <sup>1</sup>	0.72	-	see Table 2
1	Length vs. age	0.41	0.43	Richardson et al. (1999)
2	Length vs. age	0.58	0.61	Richardson et al. (1999)
3	Length vs. time	0.38	1	Richardson et al. (1999)
3	Growth rate vs. temperature	0.38	1	Richardson et al. (1999)
4	Growth rate vs. length	0.65	0.55	Šiletić and Peharda (2003)
Lab	Fecundity vs. length	1	-	Trigos et al. (2018)
-	Length vs. age <sup>2</sup>	0.58	-	Kožul et al. (2012)

\* Largest recorded individual had 120 cm, reported in Zavodnik et al. (1991).

<sup>1</sup> The ultimate size used to estimate  $f$ , 86 cm, was taken from Richardson et al. (1999).

225 *3.2. Simulation of life history traits, growth and reproduction*

226 The fitting procedure captured the observed life history traits well (Table 2). Initial energy content of  
227 an egg, length at birth, and lifespan were close to observed values, while ultimate length and gonadoso-  
228 matic index (GSI) were slightly underestimated. Age at metamorphosis and puberty were underestimated,  
229 and the corresponding length was overestimated, especially at metamorphosis.

230 Simulations successfully reproduced growth of adults (Fig. 2a) and young individuals (Fig. 2c). As  
231 expected, growth rate decreased with size (Fig. 2b), and for both 1- and 2- year old specimens increased  
232 with temperature (Fig. 2d). The model also captured positive correlation between size of the organism  
233 and its fecundity (Fig. 2e).

234 *3.3. Validation of the model*

235 Simulations agree well with independent growth data used for validation (Fig. 2f). Inclusion of water  
236 temperature corresponding to sampling area facilitated prediction of variable growth throughout the year,  
237 accurately capturing growth peak during warm, and growth stagnation during cold seasons. Consequently,  
238 validation suggests that the physiology of *P. nobilis* is well captured by the obtained parameter set.

239 *3.4. Prediction of growth and reproduction for a range of food availability*

240 The predictions of *P. nobilis* growth, maturity, energy allocated for reproduction, and fecundity for a  
241 period of 27 years at four food levels are presented in Fig. 3. As expected at abundant food ( $f = 1$ ), the  
242 bivalve grows and matures the fastest, reaches puberty after 373 days at length of 20.6 cm, and has the  
243 ultimate length of 110 cm (Fig. 3a and 3b, black dashed line). Lowering the food to the common level  
244 of wild populations ( $f = 0.72$ ), ultimate size and fecundity decreased 28% and 60%, respectively, while  
245 time to reach puberty increased about 25%, compared to the abundant food (Fig. 3a and 3b, red line vs.  
246 black dashed line; Fig. 3d, red dots vs. black crosses). Size at maturation was least impacted, decreasing  
247 only 1%. For  $f = 0.3$ , maturity was reached after approx. 3 years at size of 19.5 cm (Fig. 3b, orange  
248 dash-dotted line), and the reproduction output was 96% lower compared to abundant food (Fig. 3d,  
249 orange diamonds vs. black crosses). For  $f < 0.164$ , the ultimate size of the bivalve was 16.6 cm, they  
250 never reached puberty, and did not reproduce (Fig. 3, blue dotted line and blue 'x' markers).

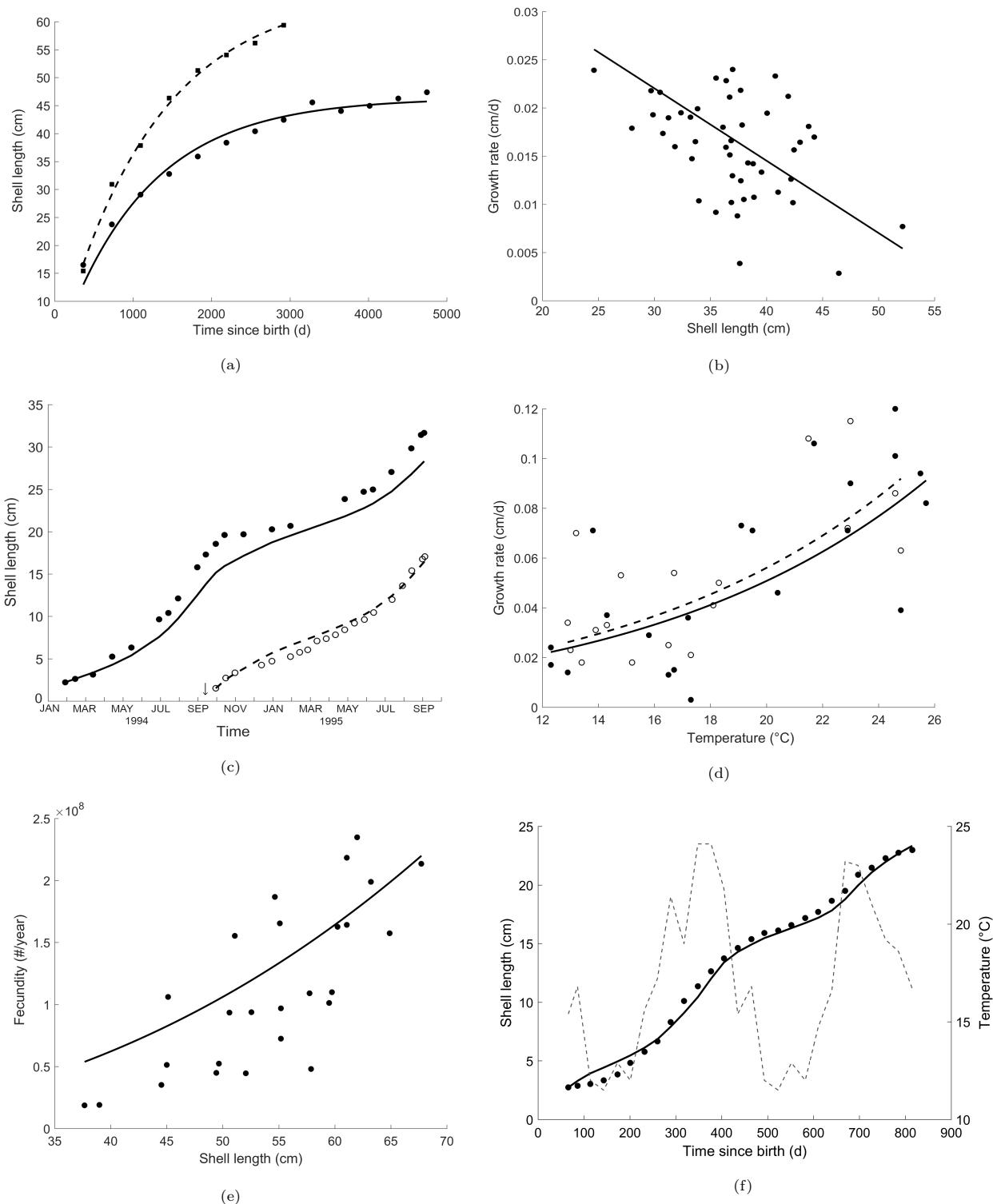


Figure 2: Observed data (markers) and model simulations (lines) for *Pinna nobilis* using a typified *abj* DEB model. (a) Shell length vs. age for populations in Aguamarga (●, —) and Carboneras (■, - -), Spain. (b) Growth rate vs. time for population in Mljet, Croatia. (c) Length vs. time and (d) temperature vs. growth rate for 2-year old (●, —) and 1-year old (○, - -) individual from Villaricos, Spain. Arrow indicates assumed time of settlement of the younger bivalve. The older individual is assumed to have settled in mid-to-early autumn of the previous year. (e) Fecundity vs. shell length. (f) Validation: shell length vs. age for population in Mali Ston Bay, Croatia. Temperature (dashed line) is taken from Peharda et al. (2012). Observed data taken from: (a),(c) and (d) Richardson et al. (1999); (b) Šiletić and Peharda (2003); (e) Trigos et al. (2018); (f) Kožul et al. (2012).

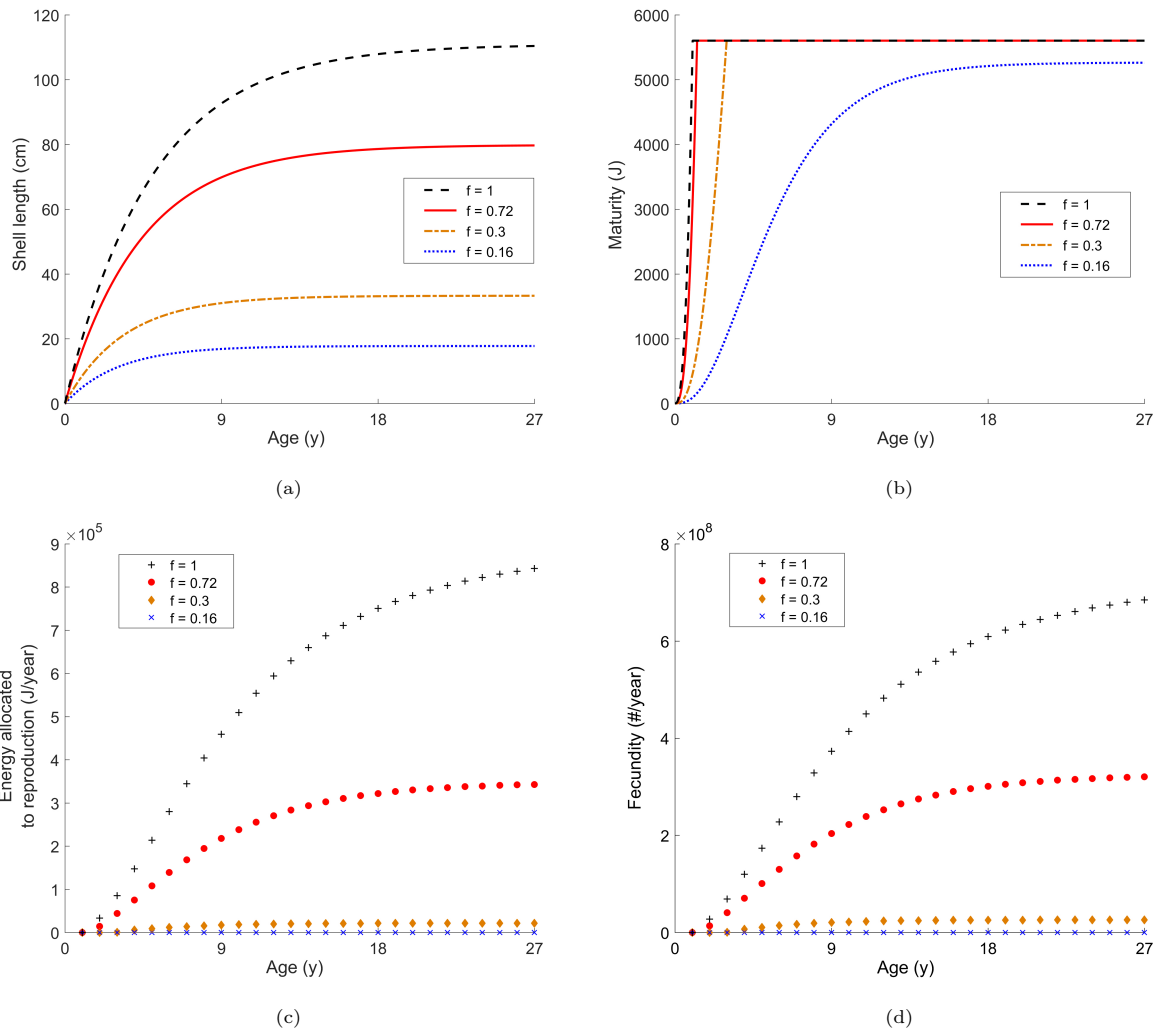


Figure 3: Predictions of growth (3a), maturation (3b), annual energy allocated for reproduction (3c) and annual fecundity (3d) of *Pinna nobilis* for a lifespan of 27 years at different food levels. Value of  $f$  ranges from the highest  $f$  that did not support reproduction ( $f = 0.16$ ) to *ad libitum* feeding ( $f = 1$ ).

251 Fecundity (Fig. 4), derived from the amount of energy allocated to reproduction (Appendix B), shows  
 252 a general positive correlation with size and functional response. However, higher number of eggs, albeit  
 253 with lower initial reserve, can be found for lower food availability. This result, counter-intuitive to the  
 254 nature of most bivalves that produce smaller amount of eggs when exposed to low food conditions,  
 255 suggests a potential modelling artefact.

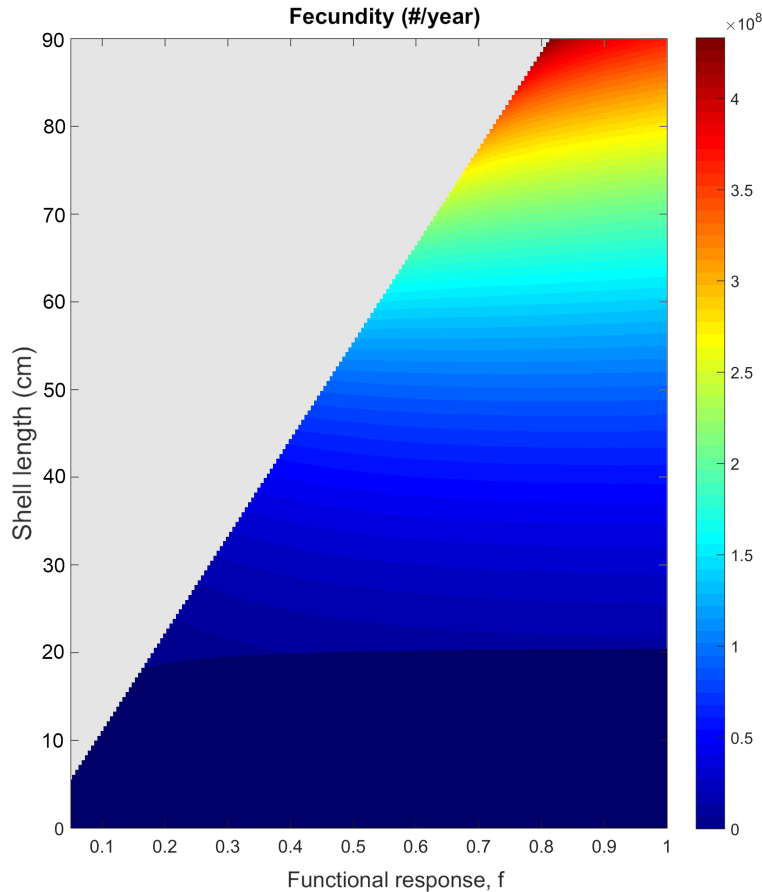


Figure 4: Fecundity (number of eggs per year) of *Pinna nobilis* depending on the bivalve size and food availability, predicted using the typified *abj* model. The gray area represents sizes greater than the maximum reachable for a given food availability. Darkest area corresponds to no reproduction. Energy required for sperm production is not included.

#### 256 4. Discussion

257 Recent mass mortality events of the critically endangered endemic Mediterranean bivalve *Pinna nobilis*  
 258 highlight the need for understanding the species' energy dynamics that could facilitate decision-making  
 259 in conservation (Riva, 2002). We created a Dynamic Energy Budget (DEB) model to capture the energy  
 260 dynamics of *P. nobilis*, and predict growth and reproduction for a range of food availability scenarios.  
 261 The key step in model development was to determine how metamorphosis should be accounted for. To

262 this end, we parameterized a standard (*std*) and a modified (typified *abj*) DEB model and compared their  
263 outputs. Additionally, we investigated effects of allometry after metamorphosis by comparing outputs of  
264 *abj* models with and without allometric growth.

265 The inclusion of allometric growth into the *abj* model had minor effect on the parameter values and  
266 on the overall model performance. Increased complexity of the model yielding practically identical results  
267 prompts us to recommend that isometric shell growth be assumed when modelling the bivalve using DEB.

268 Better performance of the typified *abj* model compared to the *std* model indicates that *P. nobilis*  
269 undergoes significant metabolic changes along with shape change during metamorphosis. The standard  
270 DEB model (Appendix A), which only accounts for change in shape, results in (i) high maximum as-  
271 similation and somatic maintenance rates, high maximum reserve density, and high development speed,  
272 with (ii) low energy conductance and low ultimate length. The typified *abj* model, on the other hand, by  
273 accounting for metabolic acceleration between birth and metamorphosis, yields a better fit to the data,  
274 and parameter values consistent with those of related species (AmP-collection, 2020; van der Veer et al.,  
275 2006; Saraiva et al., 2011; Sarà et al., 2013; Matzelle et al., 2014).

276 The acceleration of metabolism assumed by the *abj* model is consistent with physiological requirements  
277 of both planktonic and benthic stage of *P. nobilis*. Assuming mainly larval dispersal (Garstang, 1951),  
278 slow metabolism during the larval stage allows for more dispersal time (Kooijman, 2014). In contrast,  
279 higher assimilation rate after settlement optimizes organisms' ability to retain available food, a very  
280 important trait for a sessile filter feeder. The metabolic acceleration increases both assimilation and  
281 mobilisation, keeping the maximum energy density and somatic maintenance rate constant (Kooijman,  
282 2014). Increased maximum assimilation rate, combined with the relatively low somatic maintenance,  
283 supports rapid growth characteristic of *P. nobilis*.

284 Seemingly underestimated maturation age of 15 months predicted by the typified *abj* model, compared  
285 to 18 months typically observed (Richardson et al., 1999), offers insight into ontogeny of *P. nobilis*.  
286 Observed maturation age is determined by looking at *results* of a reproductive effort such as advanced  
287 gamete production or a spawning event. Maturation in DEB, however, denotes the *start* of energy  
288 investment into reproduction. Therefore, time of gonad differentiation - although also an overestimate of  
289 the true maturation time - is much closer to actual maturation than other observable physiological events  
290 (e.g. spawning). Indeed, observations of gonad differentiation coincide with DEB estimate of maturation:  
291 Deudero et al. (2017) reports differentiation starting in December, which would be 15 months after  
292 settlement assuming typical spawning and settlement pattern in Butler et al. (1993) - just as predicted  
293 by our *abj* DEB model.

294 When restricted by food, *P. nobilis* has less energy available for growth, maturation and reproduction.  
295 As a successive hermaphrodite, it will develop first male, and only later (at a larger size) female gonads  
296 (Deudero et al., 2017). Assuming male gonad development starts at 16.5 cm shell length, and female

297 gonad development at 23 cm shell length (Deudero et al., 2017), we see that *P. nobilis* will produce both  
298 male and female gametes by the time of first spawning only when food availability is high. When food  
299 availability is low, the bivalve will require an additional year to grow and start producing eggs.

300 For lower  $f$ , the model predicted smaller total energy committed to a reproductive event, smaller  
301 initial reserve per individual larvae, but higher number of offspring per individual (fecundity, Fig. 4).  
302 This apparent contradiction between higher fecundity for lower  $f$  results from the balance between size  
303 and number of offspring corresponding to the environmental conditions due to the maternal effect (Smith  
304 and Fretwell, 1974; Marshall and Uller, 2007; Segers and Taborsky, 2011). The general concept of the  
305 maternal effect in DEB is that females in environments with lower food availability produce smaller eggs  
306 that require less energy per egg (Kooijman, 2010); hence, even though total energy accumulated for  
307 reproduction is lower, number of eggs (and, therefore, fecundity), might be higher. However, in bivalves,  
308 more often than not, lower food availability results in smaller size and amount of produced eggs (Bayne  
309 et al., 1978 cf. McEdward and Miner, 2003), suggesting that for *P. nobilis* higher fecundity found at  
310 lower food availability could be a modelling artefact. Predictions agree with observations that lower  $f$   
311 leads to smaller initial reserves for larvae. Lack of food could, therefore, impact the early developmental  
312 phase of the bivalve, reducing its survival (Bayne, 1976; Helm et al., 2004), overall recruitment, and -  
313 consequently - viability of the population.

314 Results support the idea that environmental food level ( $f$ ) can be estimated as a ratio of site specific  
315 ultimate size and overall maximal size of the species. The initial estimates coincide with fitted  $f$  for three  
316 out of four sampling sites, with one estimate significantly lower than the fitted value. The corresponding  
317 site has, however, been under intense anthropogenic influence: severe trawling and collection of *P. nobilis*  
318 specimens have been reported (Richardson et al., 1999), implying that human activities, rather than food,  
319 constrained the ultimate size of the bivalves. We therefore conclude that the size-based food estimation  
320 method is reliable when applied to non-disturbed locations where food is the main limiting factor, but is  
321 of limited utility in areas where anthropogenic pressures prevail.

322 Food quality, not just quantity, could have effects on the ontogeny of *P. nobilis*. For simplicity,  
323 we assumed all individuals assimilated food of the same quality; this is, however, typically not the  
324 case. Small *P. nobilis* individuals ingest detritus of higher organic content than larger ones, who mostly  
325 predate on phyto- and zooplankton (Davenport et al., 2011). Hence, size-differential feeding may have  
326 to be considered when incorporating our model into ecological models, especially when modelling food  
327 competition between different life stages. Disturbances such as coastal discharge, algal blooms, and  
328 sediment re-suspension may influence the amount of available food for different size groups, support or  
329 limit their performance, and impact population structure. The effects of food quality can readily be  
330 incorporated into the DEB model by changing assimilation efficiency or a related parameter.

331 Temperature affects gonad maturation, onset of spawning, and survival during early development

332 (Basso et al., 2015a; Deudero et al., 2017). The optimal temperature for growth of *P. nobilis* is 20 °C, with  
333 reproductive processes regulated by seasonal fluctuations between 16 °C and 25 °C (Trigos et al., 2015).  
334 In the Mediterranean, temperatures range from 13 °C in winter to 27 °C in summer, which stresses the  
335 bivalve at both extremes. Since the Mediterranean is a climate change hot-spot (Giorgi, 2006), extreme  
336 temperatures are - especially in shallow coastal areas - expected to increase in severity and frequency,  
337 thus posing additional stress on the bivalve (Basso et al., 2015b). Our model, by quantifying effects of  
338 changing temperature on growth and reproduction, enables forecasting of effects of climate change, and  
339 identification of potential problems facing the population as environmental conditions continue to evolve.

340 Characterised by slow population dynamics and low population recruitment (Cabanellas-Reboredo  
341 et al., 2019), *P. nobilis* has limited capacity to overcome negative impacts. Current conservation sta-  
342 tus of the species requires employment of efficient conservation measures relying on (i) the ability to  
343 cultivate individuals *ex situ* and reintroducing them into the wild, and (ii) effective protection of still  
344 intact wild populations (Kersting et al., 2019). The cultivation and reintroduction efforts, as well as  
345 wild population management, can benefit from predictions of how rearing and environmental conditions  
346 dictate the performance of an individual and populations. The developed DEB model can facilitate such  
347 predictions. As a standalone tool, the model can predict how organisms individually respond to potential  
348 rearing conditions, and help optimise cultivation scenarios. The model can also help in selecting the most  
349 appropriate individuals for cultivation and reintroduction, depending on the environmental conditions at  
350 the reintroduction site.

351 Inclusion of DEB into population models is valuable because physiological processes of an individual  
352 ultimately significantly affect the population dynamics. DEB can be implemented into various population  
353 modelling approaches, such as matrix models (Klanjscek et al., 2006), individual-based models (Martin  
354 et al., 2012) and integral projection models (Smallegange et al., 2017). As a modelling building block,  
355 DEB incorporates biological realism of individual's functioning into population dynamics, with the ability  
356 to extrapolate individual changes to untested and dynamic environments (Jager et al., 2014; Marn et al.,  
357 2020).

358 The presented DEB model can be extended to include additional environmental factors. Given its  
359 large size, *P. nobilis* requires high oxygen levels, and is therefore sensitive to hypoxia. This is especially  
360 pronounced in enclosed shallow lagoons where high water temperatures facilitate oxygen depletion, and  
361 can cause collapse of dense populations (Trigos et al., 2015). Inclusion of dissolved oxygen into the model  
362 might improve the model performance and therefore give more reliable predictions. Since energy uptake  
363 appears to be the process most sensitive to hypoxia (Thomas et al., 2019), the resulting effects of oxygen  
364 availability on reserve dynamics, growth, and reproduction, can be accounted for by applying a correction  
365 factor to the ingestion rate, as demonstrated for a related bivalve *Crassostrea gigas* (Thomas et al., 2019).  
366 Another factor of potential interest is seawater pH, which is strongly affected by climate change. Within

367 DEB, impact of pH on metabolism has been explored to some degree (Muller and Nisbet, 2014), and  
368 applied to bivalves by adjusting relevant parameters to fit the data from impacted conditions (Klok et al.,  
369 2014). For *P. nobilis*, effects of low pH (i.e. acidification) are still understudied. However, for such a  
370 large calcifying organism, negative effects on physiological performance, metabolism, and calcification  
371 processes are likely, and may have to be accounted for in the future.

## 372 5. Conclusion

373 In this study, we used Dynamic Energy Budget (DEB) theory as a framework for creating a mech-  
374 anistic bioenergetic full life cycle model for critically endangered and protected Mediterranean endemic  
375 species, *Pinna nobilis*. Using only literature data, and corresponding environmental temperature and  
376 food availability, we successfully parameterized the model accounting for morphological and metabolic  
377 metamorphosis. The model resulted in realistic predictions of growth, maturation and reproduction at  
378 various food levels. Model can readily incorporate other relevant environmental factors, such as oxygen  
379 and pH. Finally, the implementation of the DEB model into population and ecosystem models can trans-  
380 late individual responses into population and ecosystem dynamics, developing a guiding tool for effective  
381 conservation decision-making.

## 382 Acknowledgment

383 The authors would like to thank S.A.L.M. Kooijman and M. Jusup for helpful advice during this  
384 research. I. Haberle was funded by Croatian Science Foundation through *Young Researchers' Career*  
385 *Development Project*. This work has been fully supported by Croatian Science Foundation under the  
386 project IP-2018-01-3150-AqADAPT.

## 387 References

- 388 AmP-collection, 2020. [http://www.bio.vu.nl/thb/deb/deblab/add\\_my\\_pet/species\\_list.html](http://www.bio.vu.nl/thb/deb/deblab/add_my_pet/species_list.html). Ac-  
389 cessed on 6.1.2020.
- 390 Basso, L., Hendriks, I.E., Duarte, C.M., 2015a. Juvenile pen shells (*Pinna nobilis*) tolerate acidification  
391 but are vulnerable to warming. *Estuaries and Coasts* 38, 1976–1985.
- 392 Basso, L., Vázquez-Luis, M., García-March, J.R., Deudero, S., Alvarez, E., Vicente, N., Duarte, C.M.,  
393 Hendriks, I.E., 2015b. The pen shell, *Pinna nobilis*: A review of population status and recommended  
394 research priorities in the Mediterranean Sea. *Advances in Marine Biology* 71, 109–160.
- 395 Bayne, B., 1976. *Marine mussels: their ecology and physiology*. Cambridge University Press, Cambridge.

- 396 Bayne, B., Holland, D., Moore, M., Lowe, D., Widdows, J., 1978. Further studies on the effects of stress  
397 in the adult on the eggs of *Mytilus edulis*. Journal of the Marine Biological Association of the United  
398 Kingdom 58, 825–841.
- 399 Butler, A., Vicente, N., De Gaulejac, B., 1993. Ecology of the pterioid bivalves *Pinna bicolor* Gmelin  
400 and *Pinna nobilis* L. Marine Life 3, 37–45.
- 401 Cabanellas-Reboredo, M., Deudero, S., Alós, J., Valencia, J., March, D., Hendriks, I.E., Álvarez, E.,  
402 2009. Recruitment of *Pinna nobilis* (Mollusca: Bivalvia) on artificial structures. Marine Biodiversity  
403 Records 2.
- 404 Cabanellas-Reboredo, M., Vazquez-Luis, M., Mourre, B., Álvarez, E., Deudero, S., Amores, A., Addis,  
405 P., Ballesteros, E., Barrajon, A., Coppa, S., et al., 2019. Tracking a mass mortality outbreak of pen  
406 shell *Pinna nobilis* populations: A collaborative effort of scientists and citizens. Scientific Reports 9,  
407 1–11.
- 408 Carella, F., Aceto, S., Pollaro, F., Miccio, A., Iaria, C., Carrasco, N., Prado, P., De Vico, G., 2019. A  
409 mycobacterial disease is associated with the silent mass mortality of the pen shell *Pinna nobilis* along  
410 the Tyrrhenian coastline of Italy. Scientific Reports 9, 2725.
- 411 Cooke, S.J., Sack, L., Franklin, C.E., Farrell, A.P., Beardall, J., Wikelski, M., Chown, S.L., 2013. What is  
412 conservation physiology? Perspectives on an increasingly integrated and essential science. Conservation  
413 Physiology 1, cot001.
- 414 Davenport, J., Ezgeta-Balić, D., Peharda, M., Skejić, S., Ninčević-Gladan, v., Matijević, S., 2011. Size-  
415 differential feeding in *Pinna nobilis* l.(Mollusca: Bivalvia): exploitation of detritus, phytoplankton and  
416 zooplankton. Estuarine, Coastal and Shelf Science 92, 246–254.
- 417 De Gaulejac, B., 1993. Etude écophysiological du mollusque bivalve méditerranéen *Pinna nobilis* L.  
418 Reproduction; Croissance; Fespiration. Ph.D. thesis. L'Université d'Aix-Marseille.
- 419 Deudero, S., Grau, A., Vázquez-Luis, M., Alvarez, E., Alomar, C., Hendriks, I., 2017. Reproductive  
420 investment of the pen shell *Pinna nobilis* Linnaeus, 1758 in Cabrera National Park (Spain). Mediter-  
421 ranean Marine Science 18, 271–284.
- 422 Deudero, S., Vázquez-Luis, M., Álvarez, E., 2015. Human stressors are driving coastal benthic long-lived  
423 sessile fan mussel *Pinna nobilis* population structure more than environmental stressors. PloS One 10,  
424 e0134530.
- 425 Galinou-Mitsoudi, S., Vlahavas, G., Papoutsi, O., 2006. Population study of the protected bivalve *Pinna*  
426 *nobilis* (Linnaeus, 1758) in Thermaikos Gulf (north Aegean Sea). Journal of Biological Research 5,  
427 47–53.

- 428 Garcia-Marsh, J.R., Vicente, N., 2006. Management tool: Management guide for marine protected areas  
429 - Protocol to study and monitor *Pinna nobilis* populations within Marine Protected Areas. MedPAN-  
430 Interreg IIIC - project, MEPA. Floriana, Malta.
- 431 Garstang, W., 1951. Larval Forms, with Other Zoological Verses. Basil Blackwell, Oxford, England.
- 432 Giorgi, F., 2006. Climate change hot-spots. Geophysical Research Letters 33, L08707.
- 433 Gómez-Alba, J., 1988. Guía de Campo de los Fósiles de España y de Europa. Omega, Barcelona, Spain.
- 434 Helm, M.M., Bourne, N., Lovatelli, A., 2004. Hatchery culture of bivalves: a practical manual. FAO.  
435 Rome, Italy.
- 436 Ijima, H., Jusup, M., Takada, T., Akita, T., Matsuda, H., Klanjscek, T., 2019. Effects of environmental  
437 change and early-life stochasticity on pacific bluefin tuna population growth. Marine Environmental  
438 Research 149, 18–26.
- 439 Jager, T., Barsi, A., Hamda, N.T., Martin, B.T., Zimmer, E.I., Ducrot, V., 2014. Dynamic energy  
440 budgets in population ecotoxicology: Applications and outlook. Ecological Modelling 280, 140–147.
- 441 Jusup, M., Sousa, T., Domingos, T., Labinac, V., Marn, N., Wang, Z., Klanjšček, T., 2017. Physics of  
442 metabolic organization. Physics of Life Reviews 20, 1–39.
- 443 Katsanevakis, S., 2005. Population ecology of the endangered fan mussel *Pinna nobilis* in a marine lake.  
444 Endangered Species Research 1, 51–59.
- 445 Katsanevakis, S., Poursanidis, D., Issaris, Y., Panou, A., Petza, D., Vassilopoulou, V., Chaldaïou, I., Sini,  
446 M., 2011. “Protected” marine shelled molluscs: thriving in Greek seafood restaurants. Mediterranean  
447 Marine Science 12, 429–438.
- 448 Katsanevakis, S., Thessalou-Legaki, M., Karlou-Riga, C., Lefkaditou, E., Dimitriou, E., Verriopoulos, G.,  
449 2007. Information-theory approach to allometric growth of marine organisms. Marine Biology 151,  
450 949–959.
- 451 Kersting, D., Benabdi, M., Čížmek, H., Grau, A., Jimenez, C., Katsanevakis, S., Öztürk, B., Tuncer, S.,  
452 Tunesi, L., Vázquez-Luis, M., Vicente, N., Otero Villanueva, M., 2019. *Pinna nobilis*. The IUCN Red  
453 List of Threatened Species .
- 454 Klanjscek, T., Caswell, H., Neubert, M.G., Nisbet, R.M., 2006. Integrating dynamic energy budgets into  
455 matrix population models. Ecological Modelling 196, 407–420.
- 456 Klok, C., Wijsman, J.W., Kaag, K., Foekema, E., 2014. Effects of CO<sub>2</sub> enrichment on cockle shell growth  
457 interpreted with a dynamic energy budget model. Journal of Sea Research 94, 111–116.

- 458 Kooijman, S.A.L.M., 2010. Dynamic Energy Budget theory for metabolic organisation. Cambridge Univ.  
459 Press, Cambridge.
- 460 Kooijman, S.A.L.M., 2014. Metabolic acceleration in animal ontogeny: an evolutionary perspective.  
461 Journal of Sea Research 94, 128–137.
- 462 Kožul, V., Glavić, N., Bolotin, J., Antolović, N., 2012. Growth of the fan mussel *Pinna nobilis* (Linnaeus,  
463 1758) (Mollusca: Bivalvia) in experimental cages in the South Adriatic Sea. Aquaculture Research 44,  
464 31–40.
- 465 Lika, K., Kearney, M.R., Freitas, V., van der Veer, H.W., van der Meer, J., Wijsman, J.W., Pecquerie,  
466 L., Kooijman, S.A.L.M., 2011. The “covariation method” for estimating the parameters of the standard  
467 dynamic energy budget model I: Philosophy and approach. Journal of Sea Research 66, 270–277.
- 468 Marin, F., Narayanappa, P., Motreuil, S., 2011. Acidic shell proteins of the mediterranean fan mussel  
469 *Pinna nobilis*, in: Müller, W.E.G. (Ed.), Molecular Biomineralization. Springer, pp. 353–395.
- 470 Marn, N., Jusup, M., Kooijman, S., Klanjšček, T., 2020. Quantifying impacts of plastic debris on marine  
471 wildlife identifies ecological breakpoints. Ecology Letter , to appear.
- 472 Marn, N., Kooijman, S., Jusup, M., Legović, T., Klanjšček, T., 2017. Inferring physiological energetics  
473 of loggerhead turtle (*Caretta caretta*) from existing data using a general metabolic theory. Marine  
474 Environmental Research 126, 14–25.
- 475 Marques, G.M., Augustine, S., Lika, K., Pecquerie, L., Domingos, T., Kooijman, S.A.L.M., 2018. The  
476 AmP project: Comparing species on the basis of dynamic energy budget parameters. PLOS Compu-  
477 tational Biology 14, 1–23.
- 478 Marques, G.M., Lika, K., Augustine, S., Pecquerie, L., Kooijman, S.A., 2019. Fitting multiple models to  
479 multiple data sets. Journal of Sea Research 143, 48 – 56.
- 480 Marshall, D.J., Uller, T., 2007. When is a maternal effect adaptive? Oikos 116, 1957–1963.
- 481 Martin, B.T., Zimmer, E.I., Grimm, V., Jager, T., 2012. Dynamic energy budget theory meets individual-  
482 based modelling: a generic and accessible implementation. Methods in Ecology and Evolution 3,  
483 445–449.
- 484 Matzelle, A., Montalto, V., Sarà, G., Zippay, M., Helmuth, B., 2014. Dynamic energy budget model  
485 parameter estimation for the bivalve *Mytilus californianus*: Application of the covariation method.  
486 Journal of Sea Research 94, 105–110.

- 487 McEdward, L.R., Miner, B.G., 2003. Fecundity-time models of reproductive strategies in marine benthic  
488 invertebrates: fitness differences under fluctuating environmental conditions. *Marine Ecology Progress*  
489 *Series* 256, 111–121.
- 490 Muller, E.B., Nisbet, R.M., 2014. Dynamic energy budget modeling reveals the potential of future growth  
491 and calcification for the coccolithophore *Emiliana huxleyi* in an acidified ocean. *Global change biology*  
492 20, 2031–2038.
- 493 Nisbet, R.M., Jusup, M., Klanjscek, T., Pecquerie, L., 2012. Integrating dynamic energy budget (DEB)  
494 theory with traditional bioenergetic models. *Journal of Experimental Biology* 215, 892–902.
- 495 Peharda, M., Ezgeta-Balić, D., Davenport, J., Bojanić, N., Vidjak, O., Ninčević-Gladan, v., 2012. Dif-  
496 ferential ingestion of zooplankton by four species of bivalves (Mollusca) in the Mali Ston Bay, Croatia.  
497 *Marine Biology* 159, 881–895.
- 498 Prado, P., Carrasco, N., Catanese, G., Grau, A., Cabanes, P., Carella, F., García-March, J.R., Tena, J.,  
499 Roque, A., Bertomeu, E., et al., 2019. Presence of *Vibrio mediterranei* associated to major mortality  
500 in stabled individuals of *Pinna nobilis* L. *Aquaculture* , 734899.
- 501 Rabaoui, L., Zouari, S.T., Katsanevakis, S., Hassine, O.K.B., 2007. Comparison of absolute and relative  
502 growth patterns among five *Pinna nobilis* populations along the Tunisian coastline: an information  
503 theory approach. *Marine Biology* 152, 537–548.
- 504 Richardson, C.A., Kennedy, H., Duarte, C.M., Kennedy, D.P., Proud, S.V., 1999. Age and growth of  
505 the fan mussel *Pinna nobilis* from south-east Spanish Mediterranean seagrass (*Posidonia oceanica*)  
506 meadows. *Marine Biology* 133, 205–212.
- 507 Riva, A., 2002. Methodological approach of some bioenergetics parameters on *Pinna nobilis*, in: Vicente,  
508 N. (Ed.), *IOPR Premier Séminaire International sur la Grande Nacre de Méditerranée: Pinna nobilis*.  
509 Nice: Mémoires de l’Institut Océanographique Paul Ricard, pp. 91–102.
- 510 Rouanet, E., Trigos, S., Vicente, N., 2015. From youth to death of old age: the 50-year story of a *Pinna*  
511 *nobilis* fan mussel population at Port-Cros Island (Port-Cros National Park, Provence, Mediterranean  
512 Sea). *Scientific Reports of Port-Cros National Park* 29, 209–222.
- 513 Sarà, G., Palmeri, V., Montalto, V., Rinaldi, A., Widdows, J., 2013. Parameterisation of bivalve functional  
514 traits for mechanistic eco-physiological dynamic energy budget (DEB) models. *Marine Ecology Progress*  
515 *Series* 480, 99–117.
- 516 Saraiva, S., Van der Meer, J., Kooijman, S., Sousa, T., 2011. DEB parameters estimation for *Mytilus*  
517 *edulis*. *Journal of Sea Research* 66, 289–296.

- 518 Seebacher, F., Franklin, C.E., 2012. Determining environmental causes of biological effects: the need for  
519 a mechanistic physiological dimension in conservation biology. *Philosophical Transactions of the Royal*  
520 *Society B: Biological Sciences* 367, 1607–1614.
- 521 Segers, F.H., Taborsky, B., 2011. Egg size and food abundance interactively affect juvenile growth and  
522 behaviour. *Functional Ecology* 25, 166–176.
- 523 Šiletić, T., Peharda, M., 2003. Population study of the fan shell *Pinna nobilis* in Malo and Veliko Jezero  
524 of the Mljet National Park (Adriatic Sea). *Scientia Marina* 67, 91–98.
- 525 Smallegange, I.M., Caswell, H., Toorians, M.E., de Roos, A.M., 2017. Mechanistic description of pop-  
526 ulation dynamics using dynamic energy budget theory incorporated into integral projection models.  
527 *Methods in Ecology and Evolution* 8, 146–154.
- 528 Smith, C.C., Fretwell, S.D., 1974. The optimal balance between size and number of offspring. *The*  
529 *American Naturalist* 108, 499–506.
- 530 Sousa, T., Domingos, T., Kooijman, S., 2008. From empirical patterns to theory: a formal metabolic  
531 theory of life. *Philosophical Transactions of the Royal Society B: Biological Sciences* 363, 2453–2464.
- 532 Thomas, Y., Flye-Sainte-Marie, J., Chabot, D., Aguirre-Velarde, A., Marques, G.M., Pecquerie, L., 2019.  
533 Effects of hypoxia on metabolic functions in marine organisms: Observed patterns and modelling  
534 assumptions within the context of dynamic energy budget (DEB) theory. *Journal of Sea Research* 143,  
535 231–242.
- 536 Trigos, S., García-March, J., Vicente, N., Tena, J., Torres, J., 2014. Utilization of muddy detritus as  
537 organic matter source by the fan mussel *Pinna nobilis*. *Mediterranean Marine Science* 15, 667–674.
- 538 Trigos, S., García-March, J.R., Vicente, N., Tena, J., Torres, J., 2015. Respiration rates of the fan mussel  
539 *Pinna nobilis* at different temperatures. *Journal of Molluscan Studies* 81, 217–222.
- 540 Trigos, S., Vicente, N., Prado, P., Espinós, F.J., 2018. Adult spawning and early larval development of  
541 the endangered bivalve *Pinna nobilis*. *Aquaculture* 483, 102–110.
- 542 Urban, M.C., Bocedi, G., Hendry, A.P., Mihoub, J.B., Pe'er, G., Singer, A., Bridle, J., Crozier, L.,  
543 De Meester, L., Godsoe, W., et al., 2016. Improving the forecast for biodiversity under climate change.  
544 *Science* 353, aad8466.
- 545 Vafidis, D., Antoniadou, C., Voultziadou, E., Chintiroglou, C., 2014. Population structure of the protected  
546 fan mussel *Pinna nobilis* in the south Aegean Sea (eastern Mediterranean). *Journal of the Marine*  
547 *Biological Association of the United Kingdom* 94, 787–796.

- 548 Vázquez-Luis, M., Álvarez, E., Barrajon, A., García-March, J., Grau, A., Hendriks, I., Jiménez, S.,  
549 Kersting, D., Moreno, D., Pérez, M., Ruiz, J., Sánchez, J., Villalba, A., Deudero, S., 2017. S.O.S.  
550 *Pinna nobilis*: A mass mortality event in Western Mediterranean Sea. *Frontiers in Marine Science* 4,  
551 1–6.
- 552 van der Veer, H.W., Cardoso, J.F., van der Meer, J., 2006. The estimation of DEB parameters for various  
553 Northeast Atlantic bivalve species. *Journal of Sea Research* 56, 107–124.
- 554 Wikelski, M., Cooke, S.J., 2006. Conservation physiology. *Trends in Ecology & Evolution* 21, 38–46.
- 555 Zavodnik, D., Hrs-Brenko, M., Legac, M., 1991. Synopsis on the fan shell *Pinna nobilis* L. in the eastern  
556 Adriatic Sea, in: Boudouresque, C.F., Avon, M., Gravez, V. (Eds.), *Les Espèces Marines à Protéger*  
557 *en Méditerranée*. GIS Posidonie Publications, Marseilles, pp. 169—178.

# 558 Appendices

## 559 A. Standard (*std*) DEB model

560 Next to the typified dynamic energy budget (DEB) model that accounts for metabolic acceleration  
561 between birth and metamorphosis (*abj*), we also parameterized a standard (*std*) DEB model of *Pinna*  
562 *nobilis*. With this step our aim was to determine whether metamorphosis of *P. nobilis* refers only to  
563 morphological change, which can be captured by the *std* model, or there is also a metabolic change which  
564 would be overlooked by the *std* and can be captured only by the *abj* model.

565 We parameterized the *std* model using the same empirical data as described in the section 2.3. Ta-  
566 ble A.1 presents fitted parameters for *std* model, along with parameters of typified *abj* model for com-  
567 parison. Table A.2 presents observed and fitted life history traits for both *std* and typified *abj* model.  
568 Fig. A.1 presents the simulations obtained using *std* model.

569 Although statistics of goodness of fit indicated that *std* parameter set fits the data well, some obvious  
570 discrepancies exist. Lifespan, size at birth, and initial energy of an egg were close to values used for  
571 parameter estimation. However, shell length at puberty was overestimated, while remaining life history  
572 traits were underestimated (Table A.2). The *std* model is characterized by constant primary parameter  
573 values, so compared to the *abj* model, the bivalve modelled with *std* has high maximum surface-specific  
574 assimilation rate  $\{\dot{p}_{Am}\}$ , low energy conductance  $\dot{v}$ , and relatively high volume-specific somatic mainte-  
575 nance rate  $[p_M]$  throughout the life cycle. Unlike in *abj* model, higher initial assimilation in the *std* model  
576 results in (i) faster initial growth and (ii) restricted ultimate size because assimilation does not increase  
577 to exceed maintenance costs (Fig. A.1a). Since both of these effects are inconsistent with observations,  
578 we conclude that the *abj* model offers a more appropriate description of *P. nobilis* ontogeny.

Table A.1: Parameter estimates of the standard (*std*) and the typified *abj* DEB models for *Pinna nobilis*, at the reference temperature  $T_{ref} = 20^\circ\text{C}$ . Fixed (not-estimated) parameters ( $\kappa_X$ ,  $\kappa_R$ ,  $F_m$ ,  $T_{ref}$ ,  $T_A$ ) are indicated in bold.

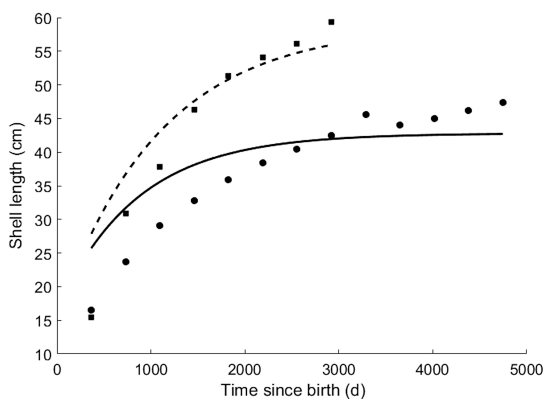
Parameter	Symbol	<i>std</i> model	typified <i>abj</i> model	Unit
Maximum surface-specific assimilation rate	$\{\dot{p}_{Am}\}$	270.06	34.74 (101.44)*	$\text{J d}^{-1} \text{cm}^{-2}$
Fraction of food energy fixed in reserve	$\kappa_X$	<b>0.80</b>	<b>0.80</b>	–
Allocation fraction to soma	$\kappa$	0.40	0.53	–
Reproduction fraction fixed in eggs	$\kappa_R$	<b>0.95</b>	<b>0.95</b>	–
Maximal surface-specific searching rate	$F_m$	<b>6.5</b>	<b>6.5</b>	$1 \text{ d}^{-1} \text{cm}^{-2}$
Energy conductance	$\dot{v}$	0.006	0.0089 (0.026)*	$\text{cm d}^{-1}$
Volume-specific somatic maintenance rate	$[\dot{p}_M]$	30.03	7.299	$\text{J d}^{-1} \text{cm}^{-3}$
Volume specific costs of structure	$[E_G]$	2346	2362	$\text{J cm}^{-3}$
Maturation threshold for birth	$E_H^b$	$9.8 \cdot 10^{-05}$	$2.9 \cdot 10^{-04}$	J
Maturation threshold for puberty	$E_H^p$	2522	5601	J
Maturity maintenance rate coefficient	$\dot{k}_J$	0.002	0.002	$\text{d}^{-1}$
Zoom factor	$z$	3.6	2.52	-
Shape coefficient (larvae)	$\delta_{M1}$	0.357	0.611	-
Shape coefficient (adult)	$\delta_{M2}$	0.035	0.066	-
Reference temperature	$T_{ref}$	<b>293.15</b>	<b>293.15</b>	K
Arrhenius temperature	$T_A$	<b>9002</b>	<b>9002</b>	K

\* The value in the brackets is the parameter value after metamorphosis (affected by acceleration factor,  $s_M = 2.92$ ).

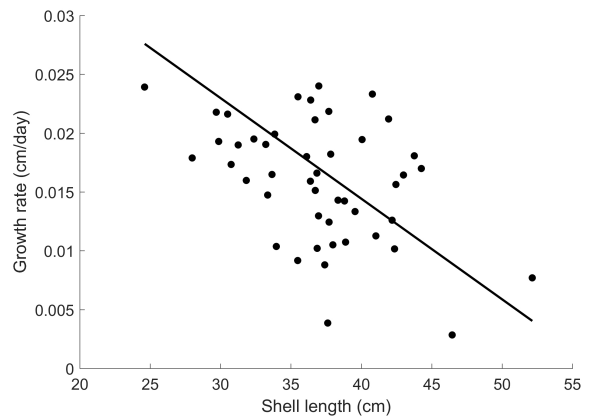
Table A.2: Observed and fitted life history traits of *Pinna nobilis* using standard (*std*) and typified *abj* DEB models at functional response value of  $f = 0.72$ . RE represents relative errors of the fitted values. Goodness of fit statistics (*std*; *abj*, respectively): MRE = 0.167; 0.202; SMSE = 0.193; 0.194. Consult Table 2 for references of observed data.

Data	Unit	Observed	<i>std</i> model		typified <i>abj</i> model	
			Fitted	RE	Fitted	RE
Age at birth	d	2	1.34	0.33	1.98	0.01
Age at puberty	y	1.5	1.24	0.17	1.26	0.15
Lifespan	y	27	27	<0.01	27	<0.01
Size at birth	cm	0.0085	0.0085	<0.01	0.0085	<0.01
Length at puberty	cm	16.5	19.95	0.21	20.18	0.22
Ultimate shell length	cm	86	74.28	0.14	79.82	0.07
Initial energy of an egg*	J	0.001	0.001	0.01	0.001	0.02
Gonadosomatic index (GSI)	-	0.52	0.50	0.04	0.48	0.08

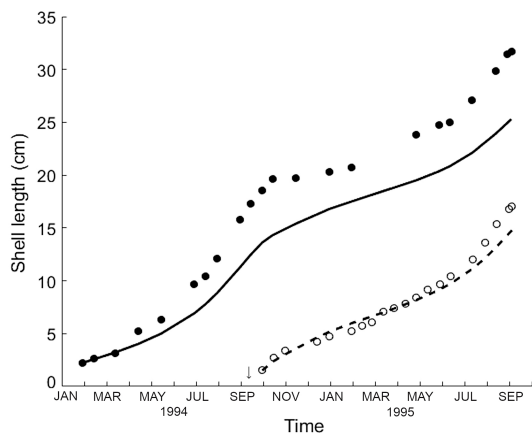
\* Data for *Crassostrea gigas*



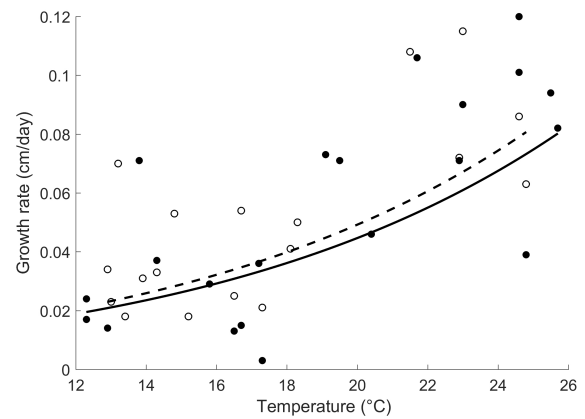
(a)



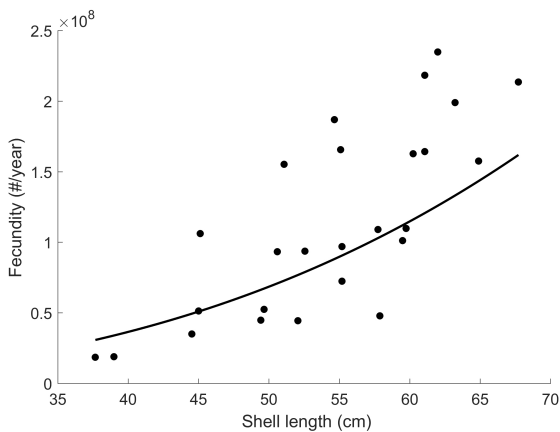
(b)



(c)



(d)



(e)

Figure A.1: Observed data (markers) and model simulations (lines) for *Pinna nobilis* using standard (*std*) DEB model. (a) Shell length vs. age for two Spanish populations, Aguamarga ( $\bullet$ ,  $-$ ) and Carboneras ( $\blacksquare$ ,  $-$ ), Spain. (b) Growth rate vs. time for population in Mljet, Croatia. (c) Length vs. time and (d) temperature vs. growth rate for 2-year old ( $\bullet$ ,  $-$ ) and 1-year old ( $\circ$ ,  $-$ ) individual from Villaricos, Spain. (e) Fecundity vs. shell length. Observed data taken from: (a),(c) and (d) Richardson et al. (1999); (b) Šiletić and Peharda (2003); (e) Trigos et al. (2018).

579 **B. Energy allocation to reproduction**

580 Energy allocation to reproduction is proportional to shell length and food availability, i.e., functional  
581 response  $f$  (Fig. B.1). Once energy allocated to reproduction (as a function of size and food availability)  
582 is known, we can also express fecundity as a function of size and food availability (Fig. 4 in the main  
583 text), while taking into account the maternal effect to calculate the initial energy in an egg.

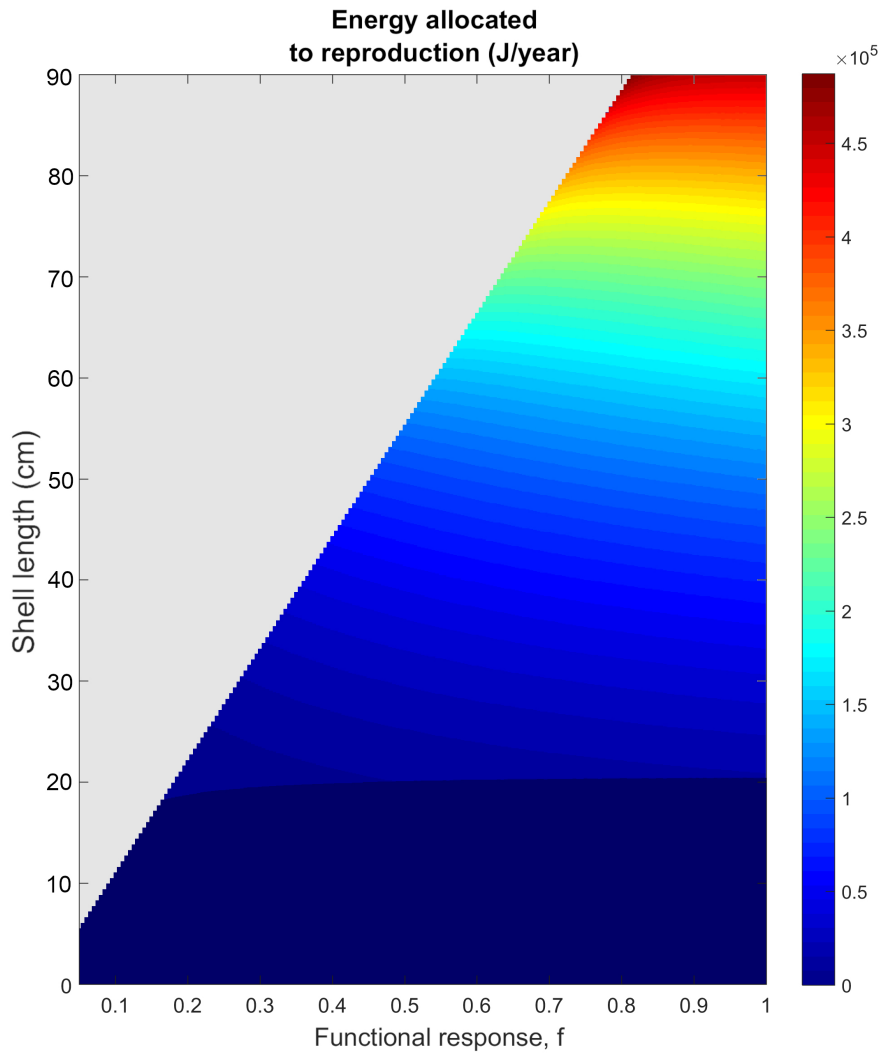


Figure B.1: Amount of energy (Joules) allocated to the reproduction of *Pinna nobilis* per year depending on the bivalve size and food availability, predicted using the typified *abj* model. The gray area represents sizes greater than the maximum reachable for a given food availability. Darkest area indicates conditions when no energy is allocated for reproduction.

584 **C. Allometric growth**

585 For each life stage, one representative morphometric dimension,  $L_w$  - chosen to accurately represent the  
 586 size of the organism, and be independent of energy reserves - is used to calculate structural length,  $L$ , and  
 587 consequently structural volume,  $V$ . When assuming isometric growth, the ratios between morphometric  
 588 dimensions are constant throughout ontogeny and the structural volume can be calculated as a cube of  
 589 structural length

$$V = L^3 = (\delta_M L_w)^3 \quad (\text{C.1})$$

590 with  $\delta_M$  as an auxiliary parameter called the shape coefficient, which accounts for proportions among the  
 591 morphometric dimensions and their relation to structural length. For *Pinna nobilis* the representative  
 592 dimension is the shell length (Figure C.1).

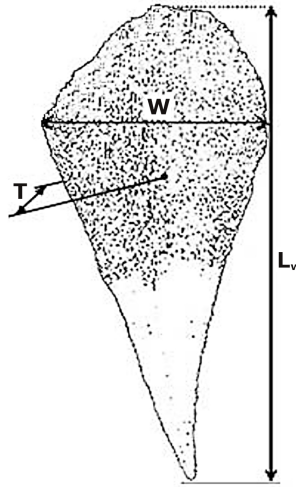


Figure C.1: The morphometric dimensions of *Pinna nobilis*.  $L_w$  - length,  $W$  - width,  $T$  - thickness. Adapted from Rabaoui et al. (2007).

593 *P. nobilis* has isometric growth during the larval phase, but it shows allometric growth after metamor-  
 594 phosis by changing the ratio between shell width and length (Katsanevakis et al., 2007; Rabaoui et al.,  
 595 2007). The allometric relation is best described with a two-segment allometric model (Katsanevakis et al.,  
 596 2007)

$$W = \begin{cases} \alpha_1 L_w^{b_1}, & L_w \leq B \\ \alpha_2 L_w^{b_2}, & L_w > B \end{cases} \quad (\text{C.2})$$

597 where  $W$  is the shell width,  $L_w$  is the shell length, and  $b_1$  and  $b_2$  are allometric exponents for each  
 598 segment. The model assumes a breakpoint  $B$ , i.e. the shell length at which positive allometry (preferential  
 599 widening) changes to negative allometry (preferential elongation). In such case, when isometric growth  
 600 is violated, and the ratios between body dimensions change as the organism grows, the structural volume

601 calculated using the Eq. C.1 may be under- or overestimated. Hence, allometric relation should be taken  
 602 into account.

603 Using the allometric relationship from Eq. C.2 we derived a new expression for calculating structural  
 604 length of *P. nobilis* after metamorphosis

$$L = \begin{cases} \delta_M L_w^{\frac{2+b_1}{3}}, & L_w \leq B \\ \beta \delta_M L_w^{\frac{2+b_2}{3}} \text{ with } \beta = B^{\frac{b_1-b_2}{3}}, & L_w > B \end{cases} \quad (\text{C.3})$$

605 where  $\delta_M$  is the shape coefficient,  $\beta$  is the normalization factor, and  $b_1$  and  $b_2$  are allometric exponents  
 606 for pre- and post-breakpoint length, respectively. Note that, at  $L_w = B$ , the following must be true:

$$\delta_M L_w^{\frac{2+b_1}{3}} = \beta \delta_M L_w^{\frac{2+b_2}{3}}. \quad (\text{C.4})$$

607 The normalization factor can be calculated from equation C.4.

608 Accounting for allometric growth after metamorphosis adds three parameters to the typified *abj* model:  
 609 the allometry breakpoint ( $B$ ), and the two allometric exponents ( $b_1$  and  $b_2$ ). Energy fluxes and state  
 610 variables are described by the same equations of the typified *abj* model (Table 1), the only difference lies  
 611 in the conversion between the representative morphometric dimension and the structural length.

612 The values of additional parameters were taken from Katsanevakis et al. (2007):  $B = 20$ ,  $b_1 = 1.2554$ ,  
 613 and  $b_2 = 0.5801$ . The final parameter set obtained by parameterization is given in Table C.1, along with  
 614 parameters of the typified *abj* model (as in Table 3), for comparison. The fit between data and model  
 615 predictions does not differ much from that obtained by the typified *abj* model (not shown), while the  
 616 added three parameters add to model complexity.

Table C.1: Parameter estimates of the *abj* DEB model accounting for allometric growth (column 3) and the typified *abj* model assuming isometric growth (column 4), for *Pinna nobilis*, at the reference temperature  $T_{ref} = 20^\circ\text{C}$ . Fixed parameters ( $B$ ,  $b_1$ ,  $b_2$ ,  $\kappa_X$ ,  $\kappa_R$ ,  $F_m$ ,  $T_{ref}$ ,  $T_A$ ) are indicated in bold. The given parameter sets result in fitted life history traits with goodness of fit (for model with; without allometry, respectively): MRE = 0.212; 0.202; SMSE = 0.201; 0.194.

Parameter	Symbol	allometry <i>abj</i> <sup>1</sup>	typified <i>abj</i> <sup>2</sup>	Unit
Allometric breakpoint*	$B$	<b>20</b>	-	cm
Allometric coefficient (pre/post breakpoint)*	$b_1 / b_2$	<b>1.2554 / 0.5801</b>	-	-
Maximum surface-specific assimilation rate	$\{\dot{p}_{Am}\}$	34.08 (94.74)**	34.74 (101.44)**	J d <sup>-1</sup> cm <sup>-2</sup>
Fraction of food energy fixed in reserve	$\kappa_X$	<b>0.80</b>	<b>0.80</b>	-
Allocation fraction to soma	$\kappa$	0.51	0.53	-
Reproduction fraction fixed in eggs	$\kappa_R$	<b>0.95</b>	<b>0.95</b>	-
Maximal surface-specific searching rate	$F_m$	<b>6.5</b>	<b>6.5</b>	l d <sup>-1</sup> cm <sup>-2</sup>
Energy conductance	$\dot{v}$	0.0087 (0.024)**	0.0089 (0.026)**	cm d <sup>-1</sup>
Volume-specific somatic maintenance rate	$[\dot{p}_M]$	6.785	7.299	J d <sup>-1</sup> cm <sup>-3</sup>
Volume specific costs of structure	$[E_G]$	2362	2362	J cm <sup>-3</sup>
Maturation threshold for birth	$E_H^b$	$3.1 \cdot 10^{-04}$	$2.9 \cdot 10^{-04}$	J
Maturation threshold for metamorphosis	$E_H^j$	$6.6 \cdot 10^{-03}$	$7.3 \cdot 10^{-03}$	J
Maturation threshold for puberty	$E_H^p$	6098	5601	J
Maturity maintenance rate coefficient	$\dot{k}_J$	0.002	0.002	d <sup>-1</sup>
Zoom factor	$z$	2.57	2.52	-
Shape coefficient (larvae)	$\delta_{M1}$	0.606	0.611	-
Shape coefficient (post metamorphosis)	$\delta_{M2}$	0.059	0.066	-
Acceleration factor	$s_M$	2.78	2.92	-
Reference temperature	$T_{ref}$	<b>293.15</b>	<b>293.15</b>	K
Arrhenius temperature	$T_A$	<b>9002</b>	<b>9002</b>	K

<sup>1</sup> Assumes isometric growth before, and allometric growth after metamorphosis.

<sup>2</sup> Assumes isometric growth both before and after metamorphosis.

\* Taken from Katsanevakis et al. (2007).

\*\* The value in the brackets is the parameter value after metamorphosis (affected by acceleration factor,  $s_M$ ).